ACS chemical biology

Letters

Cite This: ACS Chem. Biol. 2019, 14, 2160−2165

pubs.acs.org/acschemicalbiology

# $^{19}$F Paramagnetic Relaxation-Based NMR for Quaternary Structural Restraints of Ion Channels

Vasyl Bondarenko,[†] Marta M. Wells,[†] Qiang Chen,[†] Kevin C. Singewald,[#] Sunil Saxena,[#] Yan Xu,[†,§,∥,⊥] and Pei Tang*[,†,‡,§]

[†]Department of Anesthesiology and Perioperative Medicine, University of Pittsburgh, Pittsburgh, Pennsylvania 15260, United States
[‡]Department of Computational and Systems Biology, University of Pittsburgh, Pittsburgh, Pennsylvania 15260, United States
[§]Department of Pharmacology and Chemical Biology, University of Pittsburgh, Pittsburgh, Pennsylvania 15260, United States
[∥]Department of Structural Biology, University of Pittsburgh, Pittsburgh, Pennsylvania 15260, United States
[⊥]Department of Physics and Astronomy, University of Pittsburgh, Pittsburgh, Pennsylvania 15260, United States
[#]Department of Chemistry, University of Pittsburgh, Pittsburgh, Pennsylvania 15260, United States

Supporting Information

**ABSTRACT:** Quaternary distance restraints are essential to define the three-dimensional structures of protein assemblies. These distances often fall within a range of 10−18 Å, which challenges the high and low measurement limits of conventional nuclear magnetic resonance (NMR) and double electron−electron resonance electron spin resonance spectroscopies. Here, we report the use of $^{19}$F paramagnetic relaxation enhancement (PRE) NMR in combination with $^{19}$F/paramagnetic labeling to equivalent sites in different subunits of a protein complex in micelles to determine intersubunit distances. The feasibility of this strategy was evaluated on a pentameric ligand-gated ion channel, for which we found excellent agreement of the $^{19}$F PRE NMR results with previous structural information. The study suggests that $^{19}$F PRE NMR is a viable tool in extracting distance restraints to define quaternary structures.

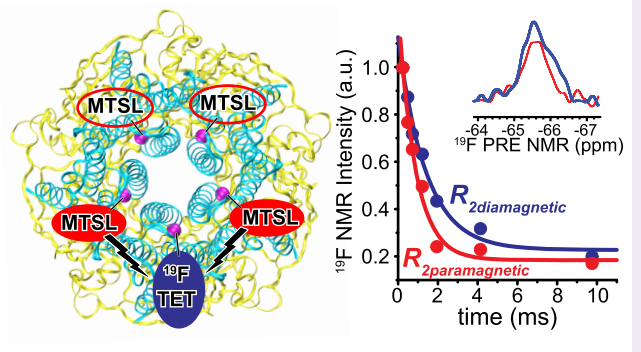


Despite great success in the use of X-ray and cryogenic electron microscopy (cryo-EM) to determine the structure of various ion channels, the capacity of these techniques to solve the structure of flexible protein regions is often challenged. Double electron−electron resonance (DEER) electron spin resonance (ESR) spectroscopy has proven to be useful for measuring quaternary structural restraints without restrictions from the local dynamic properties of ion channels.[1−5] However, for membrane proteins, DEER ESR can measure distances typically in the range of 18−60 Å and is unreliable for measuring shorter distances.[6]

Paramagnetic relaxation enhancement (PRE) in solution nuclear magnetic resonance (NMR) has been developed for extracting distance restraints of 13−25 Å between an NMR observable nucleus and a paramagnetic probe,[7−9] which is often introduced by nitroxide spin labeling of a single cysteine that exists either naturally or is introduced by mutagenesis.[10] The paramagnetic MTSL [(1-oxyl-2,2,5,5-tetramethyl-D3-pyrroline-3-methyl) methanethiosulfonate], commonly used for ESR studies, has been adopted for PRE NMR measurements. The unpaired electron spins of MTSL enhance nuclear longitudinal ($R_1$) and transverse ($R_2$) relaxation rates in a distance-dependent manner. The paramagnetic enhancement of $R_2$ in the $r^{-6}$ distance dependency for NMR nuclei within the range of 13−25 Å[7] can be quantified to extract distance information. The distances resulting from PRE measurements complement short interproton distance restraints (≤5 Å) derived from the nuclear Overhauser effect (NOE), as well as longer distance restraints measured by DEER ESR. Another benefit of PRE NMR is that it can be used to gather structural information not only for well-folded proteins but also for disordered proteins.[11] Additionally, paramagnetic probes decrease the spin−lattice relaxation time and speed up NMR data acquisition.[9] Thus, PRE NMR has become an invaluable tool in structure biology.

PRE experiments are commonly performed by monitoring $^{1}$H signal changes in $^{1}$H−$^{15}$N NMR spectra due to the MTSL-induced $R_2$ enhancement.[7,8,12,13] $^{19}$F PRE NMR,[14,15] however, has received recent attention, especially when larger proteins and protein complexes are under investigation. In general, $^{19}$F NMR is a valued addition to other structural approaches used

Received: August 28, 2019
Accepted: September 16, 2019
Published: September 16, 2019






DOI: 10.1021/acschembio.9b00692
ACS Chem. Biol. 2019, 14, 2160−2165

for characterizing structures and dynamics of proteins and protein complexes, including ion channels.[3,16−18] A null $^{19}$F signal background in native biological systems prevents signal overlap, which occurs in $^{1}$H−$^{15}$N spectra of large proteins and often compromises accurate measurements of PRE from individual sites. The excellent sensitivity of $^{19}$F resulting from its 100% natural abundance and high gyromagnetic ratio adds another advantage for using $^{19}$F PRE NMR in structure determinations.

In the present work, we have created a $^{19}$F/MTSL labeling scheme for pentameric ligand-gated ion channels (pLGICs) that allows us to determine intersubunit distances by solution $^{19}$F PRE NMR. This new strategy for gaining quaternary structural information can be easily extended to other proteins and protein complexes beyond pLGICs. A key step in acquiring this quaternary structural information via $^{19}$F PRE NMR is to label both the $^{19}$F and paramagnetic probes to selected equivalent residues in a channel complex. In our experiments, the $^{19}$F probe TET [2,2,2-trifluoroethanethiol] that provides a trifluoromethyl ($-CH_2CF_3$) was tagged to a selected cysteine in a channel protein as reported previously.[3] The paramagnetic probe MTSL was also labeled to cysteine sites equivalent to that tagged by TET. For pLGICs, a labeling molar ratio of 1 TET:4 MTSL (where one of the five subunits is labeled with TET and the remaining four subunits are labeled with MTSL) is ideal for $^{19}$F PRE NMR to extract distances between adjacent subunits. To achieve a proper TET:MTSL labeling ratio, we tested various conditions, including the order of labeling and labeling times for each species. TET has a much lower labeling efficiency than MTSL.[3] Thus, it was crucial to use an excess amount of TET as compared with MTSL. It is also important to control the total labeling time (see additional details in the Experimental Methods). The final labeling efficiencies of TET and MTSL were confirmed with respective $^{19}$F NMR and ESR,[3] showing ∼15% TET and ∼67% MTSL labeling (approximately 1:4 molar ratio) in each sample. Such labeling efficiencies ensure a sufficiently high probability of each $^{19}$F TET-labeled residue to meet at least one paramagnetic center at the equivalent residue labeled with MTSL in an adjacent subunit so that a quaternary distance restraint can be measured from $^{19}$F PRE NMR experiments.

We first examined the feasibility of this new strategy using ELIC (Figure 1a), a homomeric prokaryotic pLGIC with known X-ray structures.[19,20] In addition to the X-ray structures, DEER ESR and $^{19}$F NMR experiments were also previously performed on the ELIC L253C mutant.[3] The variety of available structural information makes the ELIC L253C construct an ideal candidate to evaluate the $^{19}$F PRE NMR strategy. Moreover, neither the TET nor the MTSL tags at L253C affect the ion channel function of ELIC.[3] Residue 253 in each ELIC subunit is located at the interface of the extracellular and transmembrane domains (Figure 1a, PDB code: 3RQU[20]). The distance between two L253 C$\beta$ atoms in the adjacent subunits is 15.3 ± 0.06 Å (mean ± standard deviation) (Figure 1b), which falls into the measurable distance range of $^{19}$F PRE NMR.[14,15] In order to know how well the distances measured through the TET and/or MTSL tags in $^{19}$F PRE NMR or DEER ESR match with the C$\beta$ distances in the X-ray structure, we modeled conformational ensembles of MTSL labels at residue 253 in the ELIC X-ray structure using MTSSLWizard software.[21] The calculated distances between the paramagnetic centers of MTSL in the adjacent subunits (18.2 ± 5.6 Å) were in excellent agreement with the experimental distance (18.5 ± 3.9 Å) measured by DEER ESR.[3] Similar MTSSLWizard calculations for TET-MTSL pairs of the adjacent residues 253 in the ELIC X-ray structure show a distance distribution (17.4 ± 4.4 Å) that also matches well with the distance derived from $^{19}$F PRE NMR described as follows.

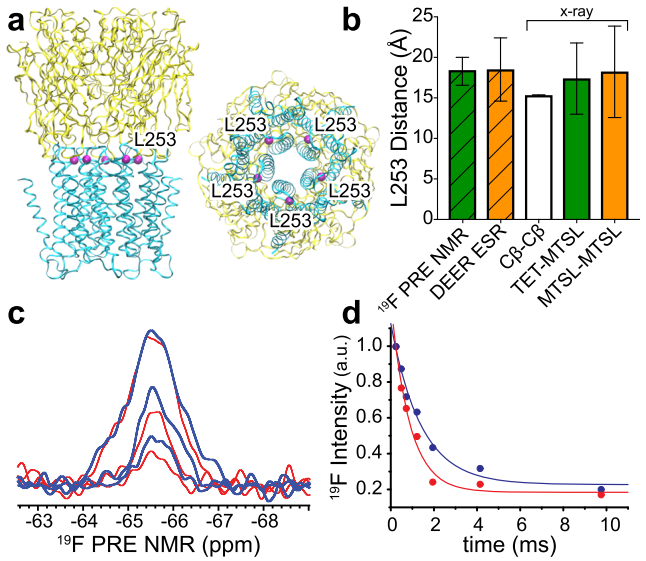


**Figure 1.** (a) Side (left) and bottom (right) views of the pentameric apo ELIC X-ray structure (PDB ID: 3RQU).[20] Five equivalent L253 residues (purple) at the interface of the extracellular domain (yellow) and the transmembrane domain (cyan) are highlighted. (b) Distances obtained from $^{19}$F PRE NMR and DEER ESR experiments are compared to distances between L253 C$\beta$ atoms (C$\beta$-C$\beta$) in adjacent subunits of the structure shown in (a). Additional comparisons include the distances between the paramagnetic center of MTSL tags (MTSL-MTSL) or the average TET fluorine positions (TET-MTSL), based on the modeled conformational ensembles of MTSL-MTSL and TET-MTSL labels in adjacent subunits of the ELIC X-ray structure using MTSSLWizard software.[21] Error bars represent standard deviation for all measured distances. (c) Representative $^{19}$F PRE NMR spectra of ELIC L253C labeled with TET and MTSL. The spectra collected under paramagnetic (red) and diamagnetic (blue) conditions with relaxation delays of 0.244 (top), 1.22 (middle), and 4.148 (bottom) ms are superimposed. (d) Normalized $^{19}$F NMR resonance intensity as a function of relaxation delay time under the paramagnetic (red) and diamagnetic (blue) conditions were fit to single exponential decay functions, resulting in transverse relaxation rates of $R_{2para}$ = 1153 ± 194 Hz and $R_{2dia}$ = 714 ± 123 Hz that were used to derive a distance of 18.4 ± 1.7 Å between residues 253 in the adjacent ELIC subunits.

$^{19}$F PRE NMR spectra of ELIC L253C labeled with TET and MTSL were collected with varied relaxation delays under paramagnetic (para) and diamagnetic (dia, after addition of ascorbic acid to the same sample) conditions (Figure 1c). The protein was solubilized in *n*-dodecyl-$\beta$-D-maltoside (DDM), which was used previously for ELIC crystal structures.[19,20] The corresponding resonance intensities ($I_{para}$, $I_{dia}$) as a function of relaxation times were fit to exponential decay functions to derive their respective transverse relaxation rates. The data collected in the paramagnetic state were fit to single, double, and triple exponential decay functions to test whether more than one $R_{2para}$ relaxation component existed in the sample. However, like $R_{2dia}$, only the single exponential decay function could fit data to generate $R_{2para}$ ($R_{2para}$ = 1153 ± 194 Hz, $R_{2dia}$



DOI: 10.1021/acschembio.9b00692
ACS Chem. Biol. 2019, 14, 2160−2165

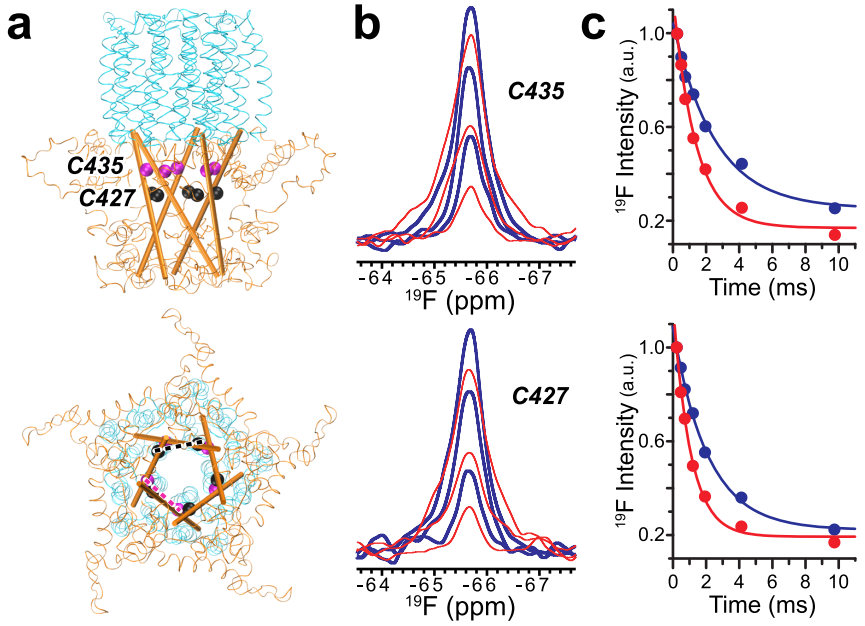


**Figure 2.** (a) Side (top) and cytoplasmic (bottom) views of the $\alpha$7 nAChR transmembrane domain (cyan) and intracellular domain (orange) showing selected residues along each intracellular MA helix (cartoon representation) for $^{19}$F PRE NMR experiments. Dashed lines highlight intersubunit distances. (b) Representative $^{19}$F PRE NMR spectra for residues C435 and C427 labeled with TET and MTSL under paramagnetic (red) and diamagnetic (blue) conditions with relaxation delays of 0.244 (top), 1.22 (middle), and 4.148 (bottom) ms. (c) Normalized resonance intensities of paramagnetic (red) and diamagnetic (blue) $^{19}$F PRE NMR spectra for residues C435 and C427 as a function of relaxation delay time. Data fitting to a single exponential decay function results in transverse relaxation rates for individual sites (C435: $R_{2para}$ = 728 ± 88 Hz and $R_{2dia}$ = 393 ± 64 Hz; C427: $R_{2para}$ = 950 ± 80 Hz and $R_{2dia}$ = 473 ± 33 Hz). Corresponding intersubunit distances were 18.3 ± 1.7 Å and 17.2 ± 1.6 Å for C435 and C427, respectively.

= 714 ± 123 Hz) (Figure 1d). A distance between the paramagnetic center of MTSL on one L253C and the fluorine atoms of TET on another L253C in the adjacent subunit of ELIC was derived on the basis of the PRE, $\Gamma_2^F = R_{2para} - R_{2dia}$, using the Solomon–Bloembergen equation:[22]

$$\Gamma_2^F = \left\{\frac{1}{15}\left(\frac{\mu_0}{4\pi}\right)^2 \gamma_F^2 g^2 \mu_B^2 S(S+1)\right\}\left\{4\tau_c + \frac{3\tau_c}{1+(\omega_F\tau_c)^2}\right\}\frac{N}{r_{F\text{-}MTSL}^6}$$

where $r$ is the distance between the $^{19}$F nucleus and the paramagnetic center, $\omega_F$ is the $^{19}$F Larmor frequency (564.68 MHz) times $2\pi$, $\tau_c$ is the correlation time for the nuclear–electron interaction that can be assumed to be equal to the global correlation time of the protein,[8] which was estimated as 218 ns at 10 °C (see Supporting Information) using Stokes' law.[23] The constants in the above equation include the permeability constant $\mu_0$, the fluorine gyromagnetic ratio $\gamma_F$, the electron g-factor $g$, the Bohr magneton $\mu_B$, and the electron spin quantum number $S$ ($S$ = 1/2) of a nitroxide radical. $N$ is the number of the paramagnetic centers adjacent to the $^{19}$F nucleus. Typically, only one paramagnetic center ($N$ = 1) is present for a chosen nucleus.[7,8,12−15] However, because of the 5-fold symmetry of homopentameric channels and the 1 TET:4 MTSL labeling scheme, the probability to have two equivalent paramagnetic centers ($N$ = 2) in the two adjacent subunits for each $^{19}$F nucleus is extremely high. Thus, we used the equation above to obtain an adjacent intersubunit distance of 18.4 ± 1.7 Å for the case of $N$ = 2. This distance is close to the predicted distance for modeled MTSL-TET pairs in adjacent ELIC subunits in the X-ray structure (Figure 1b). Small distance discrepancies from three experimental methods are expected because the intersubunit distance was measured using different reference points: C$\beta$ atoms of two adjacent L253 residues in the X-ray structure, between two adjacent MTSL paramagnetic centers in DEER ESR, or between the $^{19}$F nucleus of the labeled TET and the MTSL paramagnetic center of the adjacent subunit in $^{19}$F PRE NMR.

The 1 TET:4 MTSL labeling scheme ensures a uniform $^{19}$F PRE signal from the adjacent paramagnetic MTSL labels. However, to what degree does a nonadjacent MTSL interfere with the intended measurement for distances between adjacent subunits? The distances shown in crystal structures[19,20] and the DEER ESR results (18.5 ± 3.9 Å and 31.0 ± 5.6 Å for adjacent and nonadjacent residues 253, respectively)[3] are consistent with the geometric arrangement of a pentamer, which has a distance ratio of 1.62 between equivalent residues in nonadjacent vs adjacent subunits. A steep decay of PRE with increasing distance ($r^{-6}$) makes the PRE contribution from nonadjacent MTSL almost negligible ($(1.62)^{-6}$ < 6%). Thus, the nonadjacent subunit distance in a pentameric channel is too far to be measured by PRE and the distances extracted from the $^{19}$F PRE NMR in conjunction with our $^{19}$F/MTSL labeling scheme should predominantly reflect only the distances between adjacent subunits.

The same $^{19}$F PRE NMR strategy was applied to the human $\alpha$7 nAChR, a pentameric neurotransmitter-gated ion channel whose structures are still under investigation,[24] especially the structure of its intracellular domain. $^{19}$F PRE NMR experiments along with the 1 TET:4 MTSL labeling scheme were performed on two separate single-cysteine mutants (C435 and C427) of $\alpha$7 nAChR that are both located in the intracellular domain (Figure 2a). $^{19}$F PRE NMR spectra of C435 and C427 in micelles collected under paramagnetic (red) and diamagnetic (blue) conditions (Figure 2b) provided data to calculate the corresponding transverse relaxation rates $R_{2para}$ and $R_{2dia}$



DOI: 10.1021/acschembio.9b00692
ACS Chem. Biol. 2019, 14, 2160−2165

(Figure 2c), which allow for subsequent calculations of intersubunit distances at each residue (C435 = 18.3 ± 1.7 Å; C427 = 17.2 ± 1.6 Å). Intersubunit distances at the C435 and C427 positions are similar to distances at equivalent positions (A423 and K415, respectively) between two adjacent subunits in the cryo-EM structure (PDB code: 6BE1)[25] of the resting-state 5-$HT_{3A}$ receptor, a pentameric ligand-gated ion channel homologous to α7 nAChR (Table 1S, Supporting Information). The distances for both sites in α7 nAChR are shorter than or close to the borderline of the low distance limit of DEER ESR measurements,[6] demonstrating the value of $^{19}F$ PRE NMR as a complementary tool in quaternary structure determination.

Although the disulfide-linked labels, such as MTSL and TET, have been widely used in ESR and NMR experiments, it is reasonable to question whether these labels introduce errors to the derived distances. Indeed, one should be cautious when choosing a labeling site to avoid structural disturbance to proteins. If permitted, a functionality assessment should be arranged after labeling.[3,18] Battiste and Wagner previously showed good agreements between PRE-derived distances with an error bound of ±4 Å and the corresponding distances in a known protein structure.[7] Gottstein et al. also investigated the effect of the error margin for PRE-derived distances and found that the final structure quality was largely insensitive to the size of the error bound.[26] Structures with a backbone RMSD of 1.0−1.6 Å to the reference structure were obtained even with PRE error bounds up to 10 Å.[26] Thus, an error bound of ±4 Å for PRE-based distance restraints should ensure the structural accuracy, especially when a large number of restraints are collected from sites evenly distributed throughout the protein.

Although proteins in micelles were used in the current study, the reported method can be applied to proteins in other membrane mimics, such as nanodiscs and bicelles. The choice of membrane mimics is often determined by the protein stability and quality of NMR spectra. In most cases, membrane proteins are purified in detergent. Thus, one can complete the labeling procedures in detergent and then move the labeled protein into another mimetic membrane if it is more suitable for the protein.

Orthogonal spin labels with different spectroscopic properties have created new platforms in ESR and NMR studies of biomacromolecules with the benefit of increasing information content of experimental results.[27,28] Exploiting paramagnetic probes other than nitroxide (such as chelators of Gd(III) and other lanthanide ions) in combination with labeling to noncysteine residues (i.e., unnatural amino acids incorporated into proteins) have demonstrated great potential in various applications.[27,28] All of these options can be integrated into our reported method for extracting structural information on ion channels. For example, a $^{19}F$ probe can be introduced biosynthetically in protein expression[16] instead of chemical modification as shown in the current study. This may become more relevant if labeling of membrane-embedded cysteine is problematic. Click chemistry, which offers a fast and highly selective biocompatible reaction between azide and alkyne groups, is a good option to tag paramagnetic probes, for which unnatural amino acids can be introduced to desired sites in the protein.[28] Furthermore, one has the freedom to choose whether $^{19}F$ probe and paramagnetic tags are in equivalent or nonequivalent positions among different channel subunits. The final choice will be determined by protein performance in structural and functional experiments.

In conclusion, $^{19}F$ PRE NMR in combination with the TET/MTSL labeling scheme presented here is a realistic alternative approach for generating quaternary distance restraints for ion channels and other protein complexes that may be difficult to be defined by a different structural tool.

## EXPERIMENTAL METHODS

**Sample Preparations.** ELIC was expressed and purified as reported previously.[3,20,29] The single cysteine ELIC L253C[3] was constructed after replacing native C300 and C313 to alanine and serine, respectively, using the QuickChange Lightning Kit for single or multisite mutagenesis (Agilent Technologies). Single-cysteine α7 nAChR constructs (C427 and C435) containing the transmembrane domain (TMD) and intracellular domain (ICD) were prepared on the basis of the full-length WT α7 nAChR construct[24] by replacing native cysteines in the TMD and ICD with alanine or serine. Each construct was transformed to Rosetta (DE3) pLysS (Novagen) cells for expression in Luria−Bertani media or in the $^{15}NH_4Cl$-containing M9 media. The expression was induced with 0.2 mM isopropyl β-D-1-thiogalactopyranoside when OD reached ∼0.8. The expression at 15 °C lasted ∼24 h for ELIC or ∼72 h for the α7 nAChR TMD+ICD. Harvested cells were resuspended in a buffer (50 mM sodium phosphate at pH 8, 150 mM NaCl, and protease inhibitors for ELIC and 50 mM Tris at pH 8, 150 mM NaCl for α7) and lysed using a M-110Y microfluidizer processor (Microfluidics). The cell membrane was pelleted by ultracentrifugation. ELIC fused with maltose binding protein was extracted with 2% (w/v) DDM (Anatrace) and purified with a 5 mL HisTrap HP column (GE Healthcare). Maltose binding protein was cleaved off overnight using protease HRV3C (GE Healthcare) and separated from ELIC using HisTrap HP columns. The pentameric ELIC was collected in a buffer containing 25 mM sodium phosphate at pH 8, 125 mM NaCl, 0.05% (w/v) DDM by size exclusion chromatography using a Superdex 200 10/300 GL column (GE Healthcare). The single-cysteine α7 nAChR TMD+ICD was extracted with 2.5% (w/v) LDAO (*N*,*N*-dimethyldodecylamine *N*-oxide, Sigma) and purified with 0.4% (w/v) LDAO using a HisTrap HP column and subsequently a Superdex 200 10/300 GL column as used in ELIC purifications.

Several steps are involved in the labeling of α7 nAChR and ELIC with TET/MTSL (Toronto Research Chemicals). A given purified protein was first treated briefly (∼1 h) with the reducing reagent DTT (Invitrogen) (∼15× the protein concentration) at RT to prepare all available cysteines for labeling. After removing DTT with HiTrap Desalting columns (GE Healthcare), a 25-fold molar excess of MTSL was added to the protein and mixed with the sample for ∼30 s. Immediately after, we added a 100-fold molar excess of TET to the protein, considering that TET is more difficult to be labeled than MTSL.[3] A faster leaving group (the sulfinic acid, $CH_3SO_2H$) in the MTSL labeling process and suppressed sulfhydryl ionization that is due to a hydrophobic environment in the TET labeling sites may have contributed to their different labeling efficiencies in the channel proteins. The sample was placed on an inversion mixer and incubated for 3 h at RT and then overnight at 4 °C. Free MTSL and TET were removed by dialysis with three changes of buffer and then subjected to size exclusion chromatography on a Superdex 200 10/300 GL column. The labeling efficiencies of TET and MTSL were assessed by $^{19}F$ NMR and ESR, respectively.[3]

A typical sample for $^{19}F$ PRE NMR contained ∼100 μM protein, 20 mM sodium phosphate buffer at pH 7.7, 120 mM NaCl, and 0.5% (w/v) DDM for ELIC or 0.5−1.0% (w/v) LDAO for α7 nAChR, equivalent to a molar ratio (detergent to protein) of ∼100 for ELIC and ∼200 for α7 TMD-ICD. 5% $D_2O$ was added for deuterium lock. The diamagnetic condition for TET/MTSL-labeled samples in $^{19}F$ PRE NMR was achieved by adding a 10-fold molar excess of ascorbic acid. To determine the global rotational correlation time ($\tau_c$) of the α7 nAChR TMD+ICD by 1D [$^{15}N$−$^{1}H$]-TRACT NMR experiment,[30] a sample containing $^{15}N$-labeled α7 nAChR TMD+ICD, 5 mM sodium acetate buffer at pH 5.0, 25 mM NaCl, and 1.0% LDAO was used.



DOI: 10.1021/acschembio.9b00692
ACS Chem. Biol. 2019, 14, 2160−2165

**NMR Data Collection and Analysis.** $^{19}$F PRE NMR was performed at 10 °C on a Bruker Avance 600-MHz spectrometer ($^{19}$F frequency: 564.68 MHz) equipped with a triple-resonance $^{19}$F-detection TXO cryoprobe (Bruker Instruments). Spectra to measure the $^{19}$F transverse relaxation rates ($R_2$) were collected using the Carr−Purcell−Meiboom−Gill pulse sequence (CPMG) with 8192 data points, a 30-ppm spectral width, and a carrier frequency at −70 ppm. For each sample, spectra were collected in the absence and presence of ascorbic acid, corresponding to paramagnetic and diamagnetic conditions, respectively, with varied relaxation delays of 0.244, 0.488, 0.732, 1.22, 1.952, 4.148, and 9.76 ms and a recycle delay of 1 s. Each sample requires 24 to 30 h for NMR data collection and 9600 to 12 000 scans for each spectrum at a given relaxation delay time. The $^{19}$F chemical shift was externally referenced to the trichlorofluoromethane resonance at 0.0 ppm.

The NMR spectra were acquired, processed, and analyzed with TopSpin 3.5 (Bruker Instruments). $^{19}$F transverse relaxation rates of $R_{2para}$ and $R_{2dia}$ were obtained in the absence and presence of ascorbic acid, respectively, from fitting the $^{19}$F peak intensity ($I$) as a function of the relaxation delay in a single exponential decay function. The $^{19}$F PRE, $\Gamma_2^F = R_{2para} - R_{2dia}$, was calculated and used in the Solomon−Bloembergen equation[22] to obtain the distance between the $^{19}$F nucleus of TET in one subunit and the paramagnetic center of MTSL in the adjacent subunit.

To determine a rotational correlation time ($\tau_c$) for the $\alpha$7 nAChR TMD+ICD, a series of 1D [$^{15}$N−$^{1}$H]-TRACT NMR spectra[30] with varied relaxation periods of 0.1, 0.5, 1, 2, 4, 8, 16, 32, and 64 ms were acquired with a recycle time of 1 s at 45 °C on a Bruker Avance 700 MHz spectrometer equipped with a triple-resonance inverse-detection cryoprobe TCI (Bruker Instruments). More details for $\tau_c$ data collection and analysis are provided in Supporting Information.

## ■ ASSOCIATED CONTENT

### Supporting Information

The Supporting Information is available free of charge on the ACS Publications website at DOI: 10.1021/acschembio.9b00692.

Comparison of $^{19}$F PRE NMR measured intersubunit distances at the selected residues in $\alpha$7 nAChR with the corresponding distances measured from homologous residues in the cryo-EM structure of the resting-state 5-HT$_{3A}$ receptor (PDB code: 6BE1); methods used to determine rotational correlation time $\tau_c$ (PDF)

## ■ AUTHOR INFORMATION


### Corresponding Author

*E-mail: ptang@pitt.edu.

### ORCID

Sunil Saxena: 0000-0001-9098-6114

Pei Tang: 0000-0002-2869-2737


### Author Contributions

P.T. designed the project and wrote the manuscript with input from other authors. V.B. prepared protein and collected/analyzed NMR data. M.M.W. modeled MTSL/TET conformations in the X-ray structure of ELIC, analyzed data, and prepared figures. Q.C. participated in NMR data collection/analysis at the early stage. Y.X. contributed to the experiment design and data interpretation. K.C.S. measured MTSL labeling efficiencies using ESR with supervision from S.K.S. All authors contributed and reviewed the results and approved the final version of the manuscript.

### Notes

The authors declare no competing financial interest.

## ■ ACKNOWLEDGMENTS

The authors thank other members of the Tang laboratory and R. Ishima for helpful discussion. The research was supported by funding from NIH (R01DA046939) and NSF (MCB 1613007 and MRI 1725678). The content is solely the responsibility of the authors and does not necessarily represent the official views of the National Institutes of Health.

## ■ REFERENCES


(1) Endeward, B., Butterwick, J. A., MacKinnon, R., and Prisner, T. F. (2009) Pulsed electron-electron double-resonance determination of spin-label distances and orientations on the tetrameric potassium ion channel KcsA. *J. Am. Chem. Soc. 131*, 15246−15250.

(2) Dalmas, O., Hyde, H. C., Hulse, R. E., and Perozo, E. (2012) Symmetry-constrained analysis of pulsed double electron-electron resonance (DEER) spectroscopy reveals the dynamic nature of the KcsA activation gate. *J. Am. Chem. Soc. 134*, 16360−16369.

(3) Kinde, M. N., Chen, Q., Lawless, M. J., Mowrey, D. D., Xu, J., Saxena, S., Xu, Y., and Tang, P. (2015) Conformational Changes Underlying Desensitization of the Pentameric Ligand-Gated Ion Channel ELIC. *Structure 23*, 995−1004.

(4) Pliotas, C. (2017) Ion Channel Conformation and Oligomerization Assessment by Site-Directed Spin Labeling and Pulsed-EPR. *Methods Enzymol. 594*, 203−242.

(5) Sahu, I. D., and Lorigan, G. A. (2018) Site-Directed Spin Labeling EPR for Studying Membrane Proteins. *Biomed Res. Int. 2018*, 3248289.

(6) Jeschke, G. (2012) DEER distance measurements on proteins. *Annu. Rev. Phys. Chem. 63*, 419−446.

(7) Battiste, J. L., and Wagner, G. (2000) Utilization of site-directed spin labeling and high-resolution heteronuclear nuclear magnetic resonance for global fold determination of large proteins with limited nuclear overhauser effect data. *Biochemistry 39*, 5355−5365.

(8) Clore, G. M., and Iwahara, J. (2009) Theory, practice, and applications of paramagnetic relaxation enhancement for the characterization of transient low-population states of biological macromolecules and their complexes. *Chem. Rev. 109*, 4108−4139.

(9) Kocman, V., Di Mauro, G. M., Veglia, G., and Ramamoorthy, A. (2019) Use of paramagnetic systems to speed-up NMR data acquisition and for structural and dynamic studies. *Solid State Nucl. Magn. Reson. 102*, 36−46.

(10) Hubbell, W. L., Lopez, C. J., Altenbach, C., and Yang, Z. (2013) Technological advances in site-directed spin labeling of proteins. *Curr. Opin. Struct. Biol. 23*, 725−733.

(11) Eliezer, D. (2012) Distance information for disordered proteins from NMR and ESR measurements using paramagnetic spin labels. *Methods Mol. Biol. 895*, 127−138.

(12) Liang, B., Bushweller, J. H., and Tamm, L. K. (2006) Site-directed parallel spin-labeling and paramagnetic relaxation enhancement in structure determination of membrane proteins by solution NMR spectroscopy. *J. Am. Chem. Soc. 128*, 4389−4397.

(13) Clore, G. M., Tang, C., and Iwahara, J. (2007) Elucidating transient macromolecular interactions using paramagnetic relaxation enhancement. *Curr. Opin. Struct. Biol. 17*, 603−616.

(14) Shi, P., Li, D., Li, J., Chen, H. W., Wu, F. M., Xiong, Y., and Tian, C. L. (2012) Application of Site-Specific F-19 Paramagnetic Relaxation Enhancement to Distinguish two Different Conformations of a Multidomain Protein. *J. Phys. Chem. Lett. 3*, 34−37.

(15) Matei, E., and Gronenborn, A. M. (2016) F Paramagnetic Relaxation Enhancement: A Valuable Tool for Distance Measurements in Proteins. *Angew. Chem., Int. Ed. 55*, 150−154.

(16) Kitevski-LeBlanc, J. L., and Prosser, R. S. (2012) Current applications of 19F NMR to studies of protein structure and dynamics. *Prog. Nucl. Magn. Reson. Spectrosc. 62*, 1−33.

(17) Larda, S. T., Simonetti, K., Al-Abdul-Wahid, M. S., Sharpe, S., and Prosser, R. S. (2013) Dynamic equilibria between monomeric and oligomeric misfolded states of the mammalian prion protein measured by 19F NMR. *J. Am. Chem. Soc. 135*, 10533−10541.




DOI: 10.1021/acschembio.9b00692
*ACS Chem. Biol.* 2019, 14, 2160−2165

(18) Kinde, M. N., Bondarenko, V., Granata, D., Bu, W., Grasty, K. C., Loll, P. J., Carnevale, V., Klein, M. L., Eckenhoff, R. G., Tang, P., and Xu, Y. (2016) Fluorine-19 NMR and computational quantification of isoflurane binding to the voltage-gated sodium channel NaChBac. *Proc. Natl. Acad. Sci. U. S. A. 113*, 13762−13767.
(19) Hilf, R. J., and Dutzler, R. (2008) X-ray structure of a prokaryotic pentameric ligand-gated ion channel. *Nature 452*, 375−379.
(20) Pan, J., Chen, Q., Willenbring, D., Yoshida, K., Tillman, T., Kashlan, O. B., Cohen, A., Kong, X. P., Xu, Y., and Tang, P. (2012) Structure of the pentameric ligand-gated ion channel ELIC cocrystallized with its competitive antagonist acetylcholine. *Nat. Commun. 3*, 714.
(21) Hagelueken, G., Ward, R., Naismith, J. H., and Schiemann, O. (2012) MtsslWizard: In Silico Spin-Labeling and Generation of Distance Distributions in PyMOL. *Appl. Magn. Reson. 42*, 377−391.
(22) Solomon, I., and Bloembergen, N. (1956) Nuclear Magnetic Interactions in the Hf Molecule. *J. Chem. Phys. 25*, 261−266.
(23) Cavanagh, J., Fairbrother, W., Palmer, A. I., Rance, M., and Skelton, N. (1996) *Protein NMR Spectroscopy: Principles and Practice*, Academic Press, San Diego.
(24) Tillman, T. S., Alvarez, F. J., Reinert, N. J., Liu, C., Wang, D., Xu, Y., Xiao, K., Zhang, P., and Tang, P. (2016) Functional Human alpha7 Nicotinic Acetylcholine Receptor (nAChR) Generated from Escherichia coli. *J. Biol. Chem. 291*, 18276−18282.
(25) Basak, S., Gicheru, Y., Rao, S., Sansom, M. S. P., and Chakrapani, S. (2018) Cryo-EM reveals two distinct serotonin-bound conformations of full-length 5-HT3A receptor. *Nature 563*, 270−274.
(26) Gottstein, D., Reckel, S., Dotsch, V., and Guntert, P. (2012) Requirements on paramagnetic relaxation enhancement data for membrane protein structure determination by NMR. *Structure 20*, 1019−1027.
(27) Garbuio, L., Bordignon, E., Brooks, E. K., Hubbell, W. L., Jeschke, G., and Yulikov, M. (2013) Orthogonal spin labeling and Gd(III)-nitroxide distance measurements on bacteriophage T4-lysozyme. *J. Phys. Chem. B 117*, 3145−3153.
(28) Kucher, S., Korneev, S., Tyagi, S., Apfelbaum, R., Grohmann, D., Lemke, E. A., Klare, J. P., Steinhoff, H. J., and Klose, D. (2017) Orthogonal spin labeling using click chemistry for in vitro and in vivo applications. *J. Magn. Reson. 275*, 38−45.
(29) Chen, Q., Kinde, M. N., Arjunan, P., Wells, M. M., Cohen, A. E., Xu, Y., and Tang, P. (2015) Direct Pore Binding as a Mechanism for Isoflurane Inhibition of the Pentameric Ligand-gated Ion Channel ELIC. *Sci. Rep. 5*, 13833.
(30) Lee, D., Hilty, C., Wider, G., and Wuthrich, K. (2006) Effective rotational correlation times of proteins from NMR relaxation interference. *J. Magn. Reson. 178*, 72−76.



DOI: 10.1021/acschembio.9b00692
*ACS Chem. Biol.* 2019, 14, 2160−2165